Ethylene signaling increases reactive oxygen species accumulation to drive root hair initiation in Arabidopsis

R. Emily Martin[a], Eliana Marzol[c], Jose M. Estevez[b,c], Gloria K. Muday[a*]

[a] Departments of Biology and Biochemistry and the Center for Molecular Signaling, Wake Forest University, 1834 Wake Forest Road, Winston-Salem, NC 27109

[b] Fundación Instituto Leloir and IIBBA-CONICET. Av. Patricias Argentinas 435, Buenos Aires C1405BWE, Argentina.

[c] Centro de Biotecnología Vegetal, Facultad de Ciencias de la Vida, Universidad Andres Bello and ANID - Millennium Science Initiative Program - Millennium Institute for Integrative Biology (iBio), Santiago, Chile.

*Corresponding author, email**:** muday@wfu.edu

Author Contributions: REM conceived the research plan, designed and performed experiments and data analysis and wrote the article, EM and JME designed and prepared genetic constructs and provided editorial input into the writing, GKM conceived the research plan, supervised the project, and provided editorial input into the writing.

Keywords: Ethylene, reactive oxygen species, root hairs, peroxidase, RBOH

ABSTRACT

Root hair initiation is a highly regulated aspect of root development. The plant hormone, ethylene, and its precursor, 1-amino-cyclopropane-1-carboxylic acid (ACC), induce formation and elongation of root hairs. We asked whether elevated ethylene induced root hair formation by increasing reactive oxygen species (ROS) synthesis in hair cells. Using confocal microscopy paired with redox biosensors and dyes, we demonstrated that treatments that elevate ethylene levels led to increased ROS accumulation in hair cells prior to root hair formation. In two ethylene-insensitive mutants, *etr1-3* and *ein3/eil1*, there was no increase in root hair number or ROS accumulation. Conversely, *etr1-7,* a constitutive ethylene signaling receptor mutant, has increased root hair formation and ROS accumulation similar to ethylene-treated wild type seedlings. The *rhd2-6* mutant, with a defect in the gene encoding a ROS synthesizing Respiratory Burst Oxidase Homolog C (RBOHC) and the *prx44-2* mutant defective in a class III peroxidase, showed impaired ethylene-dependent ROS synthesis and root hair formation and decreased RBOH enzyme activity compared to Col-0. Together, these results support a model in which ethylene increases ROS accumulation through RBOHC and PRX44 to drive root hair formation.

36 **SUMMARY STATEMENT**

37 The gaseous hormone ethylene increases root hair initiation by elevating reactive oxygen species (ROS)
38 levels. Genetic and biochemical approaches identified ethylene-regulated ROS producing enzymes that
39 drive root hair initiation.

40 **INTRODUCTION**

41 The initiation of root hairs is genetically programmed and environmentally sensitive, making them
42 an ideal model for studying single cell development in plants. Root hairs are single-cell extensions that
43 differentiate from longitudinal epidermal cell files, known as trichoblasts (Leavitt, 1904; Salazar-Henao et
44 al., 2016). The formation of root hairs is modulated by environmental changes to increase root surface area
45 to allow for efficient water and nutrient uptake (Bruex et al., 2012), while also anchoring plants in soil to
46 reduce erosion (De Baets et al., 2020). In Arabidopsis, the root epidermis consists of an alternating pattern
47 of trichoblasts, which form root hairs, and atrichoblasts, which are non-hair forming cells (Pemberton et al.,
48 2001; Salazar-Henao et al., 2016). Root hair formation is dictated by cell positioning; epidermal cells
49 overlying two cortical cells can become hair forming cells, while those overlying one cortical cell will become
50 non-hair cells (Berger et al., 1998; Salazar-Henao et al., 2016). Root hair development is separated into
51 two processes: root hair initiation and root hair elongation (Dolan et al., 1994), although a recent report
52 divided this process into 10 precise stages and examined the molecular mechanisms that drive this process.
53 During stages -7 to -1, RHO Of Plants (ROP) proteins (ROP2, ROP4, and ROP6) and ROP Guanine
54 Nucleotide Exchange factors (ROP GEFs) that regulate ROP activity accumulate at the future site of
55 initiation (Denninger et al., 2019; Molendijk et al., 2001), this is followed by actin polymerization along which
56 vesicles move to deposit membrane allowing for polarized tip growth (Salazar-Henao et al., 2016). During
57 tip growth, tip focused reactive oxygen species (ROS) (Foreman et al., 2003; Gayomba and Muday, 2020)
58 and Ca^{2+} gradients (Carroll et al., 1998) have been identified to drive exocytosis of the cell wall and
59 membrane materials driving subsequent root hair elongation. These processes are separable as mutants
60 with impaired root hair initiation or elongation have been identified (Masucci and Schiefelbein, 1994;
61 Schiefelbein and Somerville, 1990)

62 Genetic screens in *Arabidopsis thaliana* have provided a wealth of insight into the proteins that
63 drive root hair development (Lee and Schiefelbein, 1999; Masucci and Schiefelbein, 1996; Rerie et al.,
64 1994). For example, the mutants *transparent testa glabra (ttg)*, *glabra2 (gl2)*, and *werewolf (wer)* have root
65 hairs that form from both trichoblast and atrichoblast cells (Di Cristina et al., 1996; Galway et al., 1994; Lee
66 and Schiefelbein, 1999). Many of the protein products of these mutants have been mapped to

67 transcriptional cascades that drive root hair differentiation (Shibata and Sugimoto, 2019) and have been
68 shown to localize prior to root hair initiation (Denninger et al., 2019). In non-hair cells, a transcriptional
69 complex comprised of three transcription factors (TFs), WER, GLABRA 3 (GL3), or its functionally
70 redundant ENHANCER OF GLABRA (EGL3), and TTG1, function as a transcriptional activator of the GL2
71 protein, which leads to repression of root hair initiation (Grebe, 2012; Salazar-Henao et al., 2016). In
72 trichoblasts, *WER* expression is repressed, which allows for the formation of an alternate transcriptional
73 complex comprised of CAPRICE (CPC) or the functionally redundant proteins ENHANCER OF TRY AND
74 CPC1 (ETC1), ETC3, or TRYPTICHON (TRY) (Schiefelbein et al., 2014). When this pathway is active, GL2
75 is not expressed and root hair initiation proceeds (Salazar-Henao et al., 2016).

76 Another genetic screen identified the *root hair defective* (*rhd*) mutants which have impaired root
77 hair initiation, elongation or structure (Masucci and Schiefelbein, 1994; Schiefelbein and Somerville, 1990).
78 In one of these mutants, *rhd2,* the mutation was mapped to the *RBOHC* (respiratory burst oxidase homolog
79 C/NADPH oxidase) gene (Foreman et al., 2003). The *rhd2* mutant was identified for altered root hair
80 elongation (Schiefelbein and Somerville, 1990), but was recently reported to also have impaired root hair
81 formation (Gayomba and Muday, 2020). RBOHs are integral plasma membrane proteins that produce
82 superoxide, which can be dismutated to hydrogen peroxide via superoxide dismutase (SOD) or other non-
83 enzymatic mechanisms (Chapman et al., 2019). H_2O_2 can then enter into the cell through aquaporins
84 (Bienert et al., 2007), where it can act as a signaling molecule to drive cellular processes. Signaling induced
85 ROS regulates protein function by reversibly oxidizing cysteine residues to sulfenic acids (Cys-SOH) (Poole
86 and Schoneich, 2015).

87 There are 10 RBOH family members (RBOHA-RBOHJ) in Arabidopsis and each play distinct roles
88 in organ development and stress response (Chapman et al., 2019). RBOHs can be regulated
89 transcriptionally or enzymatically by a number of mechanisms, including calcium binding, phosphorylation,
90 and phosphatidic acid binding (Kobayashi et al., 2007; Postiglione and Muday, 2020; Suzuki et al., 2011).
91 RBOH-induced ROS production is also regulated by hormone signaling, as many plant hormones generate
92 ROS as a mechanism to drive growth and developmental processes (Chapman et al., 2019; Kwak et al.,
93 2003; Mittler et al., 2011; Postiglione and Muday, 2020). For example, abscisic acid (ABA), a hormone

involved in abiotic stress response, has been shown to induce RBOH-derived ROS production to prevent water loss in leaves (Kwak et al., 2003). Auxin induces root hair elongation through a localized increase in ROS (Mangano et al., 2017), suggesting that RBOH may drive hormone induced root hair elongation.

The plant hormone ethylene enhances root hair initiation and elongation. Treatment with ethylene, or its precursor 1-amino-cyclopropane-1-carboxylic acid (ACC), leads to proliferation of root hairs, with substantial increases in length (Tanimoto et al., 1995). The ethylene induction of root hairs occurs through the canonical ethylene signaling pathway, which is initiated when ethylene binds to one of the five receptors, ETR1, ERS1, ETR2, ERS2, or EIN4 (Binder, 2020; Bleecker, 1999). When ethylene is absent, the receptors are in the “on state” leading to activation of the CTR1 Raf-like kinase (Kieber et al., 1993); this turns the pathway off via phosphorylation and subsequent degradation of the EIN2 transmembrane protein (Alonso et al., 1999; Ju et al., 2012). When ethylene binds to its receptors they shift to the “off state” which prevents activation of CTR1. This allows for cleavage and translocation of the EIN2 C-terminus into the nucleus (Ju et al., 2012; Wen et al., 2012) where it stabilizes the EIN3/EIL1 TFs leading to ethylene responsive gene expression. Previous work has shown that ethylene regulates root hair elongation through the EIN3 transcription factor (Feng et al., 2017) and that EIN3 also controls the formation of ectopic root hairs when ethylene reaches very high levels (Qiu et al., 2021). EIN3 physically interacts with RHD6, a known positive regulator of root hair development, to form a transcriptional complex that binds to and induces expression *RSL4*. This transcriptional regulation results in increased root hair length (Feng et al., 2017). However, the mechanistic events that drive ethylene-induced root hair initiation have not been fully described and the role of ROS as a downstream molecule in ethylene-induced root hair development has not been reported.

We asked whether ethylene acts to increase ROS levels to drive root hair initiation. Using fluorescent dyes and biosensors that report ROS levels, we examined ROS accumulation after ethylene or ACC treatment in trichoblast cells in the differentiation zone. We asked whether this response is dependent on ETR1 receptor activity and EIN3 TF activity. We also examined the role of RBOHC and class III peroxidase enzymes in ethylene-dependent ROS synthesis. Together these experiments demonstrated that ROS is a signaling molecule in ethylene induced root hair development and identified several enzymes that participate in producing ethylene-induced ROS.

121 **RESULTS**

122 **Root hair number was increased in ACC treated roots**

123 To understand the role of ethylene signaling in root hair initiation we examined the effects of short-
124 term treatments with the ethylene precursor, ACC, on the number and position of root hairs in 5 day old
125 seedlings. Root hairs were visualized in wild type (Col-0) seedlings grown in the presence of 1 μM ACC
126 for 4 hours (Figure 1A). The root tip was divided into three 500 μm zones starting from the root tip and the
127 number of initiated root hairs (stage +2 and above as described by (Denninger et al., 2019) formed in each
128 zone was quantified Figure 1B). In zone 1, root hairs did not form in either untreated or ACC-treated
129 seedlings. In zone 2, there were very few root hairs in untreated roots, however, ACC-treatment increased
130 the number of root hairs by 10-fold. There was also a 2-fold increase in root hair number in zone 3 of ACC-
131 treated seedlings compared to untreated controls. It is also evident from Figure 1, that this treatment
132 increases the length of root hairs in both zone 2 and 3, consistent with prior reports (Feng et al., 2017;
133 Harkey et al., 2018). These data suggest that ACC-induced root hair initiation begins between 500 and
134 1000 μM from the root tip. Therefore, to understand the mechanisms driving the process of root hair
135 initiation our experiments focused on this region.

136 ACC treatment also resulted in a shorter primary root due to reduced elongation of root cells
137 (Harkey et al., 2018), therefore we asked whether the increase in root hairs seen with this brief 4 hour
138 treatment with ACC was due to shorter cell length resulting in more root hairs in zone 2. To explore this
139 possibility, roots treated with or without ACC for 4 hours were stained with the cell wall specific dye,
140 propidium iodide (PI). We then measured the length of 5 epidermal cells from 6-8 roots per treatment
141 condition, measuring the length of cells at either end and in the middle of zone 2 (designated zone 2A, 2B,
142 and 2C in Figure S1). There was no difference in cell length in any of these 3 regions after 4 hours of ACC
143 treatment compared to untreated controls. These results are consistent with short term and low dose ACC
144 treatments increasing root hair number by inducing more root hair forming trichoblasts in zone 2, rather
145 than as an indirect effect of a shorter primary root.

146 **A ROS dependent transcriptional reporter was increased in ACC treated roots**

147 We asked whether ethylene leads to elevated reactive oxygen species (ROS) to drive ethylene-
148 induced root hair initiation. We examined ROS dependent gene expression along the root using the
149 ZAT12p-ROS ratiometric biosensor (Lim et al., 2019). This reporter construct contains the promoter of the
150 ROS sensitive transcription factor, ZAT12, driving GFP and the constitutive ubiquitin10 promoter driving
151 mCherry. We compared the fluorescent signal of ZAT12p-ROS in the presence and absence of ACC as
152 visualized by laser scanning confocal microscopy (LSCM), with GFP reported as green and mCherry
153 reported as magenta (Figure 1C). The ratio of signal of GFP (green) to mCherry was quantified t across the
154 entire root as a distance from the root tip. In ACC-treated roots, the GFP/mCherry ratio increased beginning
155 at approximately 500 μm from the root tip, which corresponded to zone 2, where root hair induction was
156 maximal upon treatment with ACC (Figure 1D).

157 **Ethylene increases the signal of the H_2O_2 selective dye, Peroxy Orange1, in trichoblast cells**

158 We also used the hydrogen peroxide selective dye, Peroxy-Orange 1 (PO1), to ask whether there
159 were cell type-specific increases in ROS in response to ACC or ethylene gas. PO1 is a permeable,
160 boronate-based dye that is non-fluorescent in its reduced form, but becomes fluorescent when irreversibly
161 oxidized by H_2O_2 (Dickinson et al., 2010). We treated Col-0 seedlings with either 1 μM ACC or 0.05 ppm
162 of ethylene gas for 4 hours followed by PO1 staining. In Col-0 roots, PO1 fluorescence was visualized using
163 LSCM in zone 2 of roots treated with control, ACC, or ethylene gas for 4 hours (Figure 2). In Arabidopsis,
164 root hairs form in alternating patterns, so that every root hair forming cell (trichoblast) is adjacent to a non-
165 hair cell (atrichoblast). We quantified ROS accumulation by analyzing PO1 signal after confocal imaging,
166 by drawing a line across the width of the root that spans 5 epidermal cell files so that the PO1 signal in 3
167 trichoblasts (numbered 1, 3, and 5) and 2 atrichoblasts (numbered 2 and 4) was quantified (Figure 2A). We
168 found that PO1 accumulation in trichoblasts in zone 2 of untreated seedlings was slightly, but not
169 significantly higher than atrichoblasts. In trichoblast cells in ACC treated seedlings, there was a significant
170 increase in PO1 accumulation in ACC-treated trichoblasts as compared to trichoblasts of untreated
171 seedlings and compared to atrichoblasts of both untreated and ACC treated seedlings. In contrast, there
172 were no changes in PO1 in the atrichoblasts suggesting that ethylene and ACC treatment increased ROS
173 levels in only the cells that formed root hairs, with PO1 fluorescence intensity values in trichoblasts after

174 both treatments showing the same magnitude increase as root treated with ACC (Figure 2B). These results
175 are consistent with this short term and low dose treatment with ACC leading to efficient conversion to
176 ethylene that in turn produces elevated ROS in trichoblast cells.

177 **ROS accumulation increased prior to root hair emergence**

178 To determine whether ethylene-induced ROS accumulation drives root hair emergence, we asked
179 whether the ACC-induced ROS increases were detectable prior to the first ACC-induced root hair initiation.
180 Wild type Col-0 seedlings were treated with ACC for either 2 or 4 hours and PO1 fluorescence was
181 visualized in trichoblasts that did not have a root hair bulge (stages below +1) (Figure 3A). This PO1 signal
182 is only reported in the 2-hour ACC treatment, as there were insufficient number of cells without root hair
183 bulges to quantify in root treated for 4 hours. These trichoblasts were chosen for quantification to determine
184 whether ACC-induced ROS increases were seen in hair forming cells prior to root hair emergence. Total
185 PO1 accumulation was measured in 5 individual trichoblasts per root treated with and without ACC. Signal
186 was quantified across the area of the entire cell and the average PO1 intensity of 24-30 individual cells was
187 reported (Figure 3B). Atrichoblast signal was not quantified as ROS levels did not change in those cells
188 (Figure 2B). Cells treated with ACC for 4 hours were not quantified because nearly all of the trichoblasts in
189 Zone 2 at this time point had already begun the process of root hair initiation (Figure 3C). These data
190 showed a 1.3-fold increase in PO1 accumulation in hair cells of seedlings treated with ACC for 2h as
191 compared to untreated controls, when trichoblast cells that had not yet begun to initiate root hairs were
192 examined. These data are consistent with the hypothesis that ROS acts as a driver of root hair initiation
193 downstream of ethylene signaling.

194 **Ethylene signaling mutants showed altered ROS accumulation patterns and root hair phenotypes**

195 We examined ROS accumulation in response to ACC treatment in seedlings with mutations in
196 genes encoding key ethylene signaling proteins to ask whether this response was dependent on the
197 ethylene signaling pathway and downstream transcriptional responses. The number of root hairs and
198 average length were previously reported in loss-of-function and gain-of-function ethylene receptor mutants,
199 *etr1-7 and etr1-3,* and the transcription factor mutant *ein3eil1* in the presence and absence of ACC
200 treatment (Harkey et al., 2018). *etr1-7* is a LOF mutant in which the ETR1 receptor is inactive, therefore the

201 ethylene signaling pathway is constitutively signaling and there are increased numbers of root hairs
202 independent of ACC addition, while *etr1-3* is a GOF mutant in which the ETR1 receptor is always active
203 leading to an inactive signaling pathway (Harkey et al., 2018; Hua and Meyerowitz, 1998). The double
204 mutant *ein3eil1* has mutations in genes encoding EIN3 and EIL1 TFs (Chao et al., 1997; Solano et al.,
205 1998). Both *etr1-3* and *ein3eil1* have reduced root hair initiation in response to ACC treatment (Harkey et
206 al., 2018). We examined the PO1 distribution patterns in root hair cells with and without ACC treatment in
207 these three mutants. We visualized PO1 fluorescence via LSCM and saw that the constitutive ethylene
208 signaling mutant *etr1-7* had increased H_2O_2 in root hair cells and increased root hair initiation from these
209 cells regardless of ACC treatment (Figure 4). The opposite response was seen in the ethylene-insensitive
210 *etr1-3* and *ein3eil1* mutants, as they showed reduced PO1 signal and root hair initiation and no increase in
211 H_2O_2 accumulation in the presence of ACC. Together, these results suggest that the ETR1 receptor and
212 EIN3/EIL1 TFs are required for ethylene-induced ROS accumulation and root hair initiation.

213 **The RBOHC knockout mutant, *rhd2-6*, showed decreased ROS accumulation after ACC treatment**

214 It has been previously reported that the respiratory burst oxidase homolog C (RBOHC) is involved
215 in ROS production and subsequent root hair elongation (Foreman et al., 2003). We have also shown that
216 there is decreased ROS in root hairs of the *rhd2-6* mutant, which has an insertion mutation in the *RBOHC*
217 gene (Gayomba and Muday, 2020). Therefore, we asked whether RBOHC is required for ACC-induced
218 ROS increases and root hair initiation. We examined root hair numbers via light microscopy in ACC-treated
219 *rhd2-6* (*rbohc*) seedlings (Figure 5). Root hair number in the ACC-treated *rhd2-6* mutant was significantly
220 less than ACC-treated Col-0, suggesting that RBOHC contributes to ethylene-induced root hair initiation
221 (Figure 5B). We also quantified the length of all root hairs in Zone 2 by measuring the length of all root hairs
222 in zone 2 using the segmented line tool in ImageJ. A histogram showing the distribution of lengths of root
223 hairs (reported as percentage in each length bin out of total number of roots) revealed that the length of
224 root hairs increased after ACC treatment and that the *rhd2-6* mutant has reduced root hair elongation in the
225 presence of ACC relative to Col-0.

226 We also visualized the PO1 fluorescence by LSCM in the *rhd2-6* mutant with and without ACC
227 treatment (Figure 5D). We report the average of 2 trichoblast cells (1 and 5 from Figure 2) and two

228 atrichoblast cells (2 and 4) in Figure 5E. This method still reveals a significant increase in H_2O_2 fluorescence
229 accumulation in Col-0 hair cells, while in *rhd2-6* there is no significant increase after ACC treatment (Figure
230 5E), suggesting that RBOHC contributes to ethylene-induced ROS accumulation. The data is reported for
231 all 5 cell files in Figures S2. To determine if other RBOHs that are expressed in root tissue contributed to
232 ethylene-induced ROS accumulation, PO1 accumulation patterns were examined in the *rbohd/f* double
233 mutant and compared to *rhd2-6*. No change was seen in ROS levels in hair cells of *rbohd/f*, suggesting that
234 these RBOHs do not contribute to ethylene-induced ROS synthesis in root hair cells (Figure S2).

235 **RBOH enzyme activity was increased in response to ethylene signaling**

236 Elevated ethylene may either increase *RBOHC* transcript abundance or enzyme activity. We
237 examined several transcriptomic datasets with ACC or ethylene treated roots and found a subtle change in
238 the *RBOHC* transcripts, but not significant enough to pass the filtering on this transcriptomic analysis
239 (Harkey et al., 2018; Harkey et al., 2019) (Table S1). To determine if ethylene signaling regulated RBOH
240 enzyme activity, a spectrophotometric assay using nitro blue tetrazolium (NBT) dye as an electron acceptor,
241 was performed. NBT is reduced by superoxide to monoformazan and this reduction can be detected at 530
242 nm. This experiment was performed in protein extracts from 7-day old roots of Col-0 and *rhd2-6* treated
243 with and without ACC for 4 hours. Older roots were used in this experiment to obtain an adequate amount
244 of protein for these assays. There was a significant 2-fold increase in monoformazan production in protein
245 extracts of Col-0 roots treated with ACC for 4 hours compared to controls (Figure 5F). The enzyme activity
246 of roots of untreated *rbohc/rhd2-6* was 3-fold lower than roots of untreated Col-0 and the enzyme activity
247 in the presence of ACC was significantly reduced relative to ACC treated Col-0 (Figure 5F). These data are
248 consistent with previous results indicating that the RBOHC enzyme constitutes the majority of the
249 superoxide production in roots (Chapman et al., 2019; Gayomba and Muday, 2020).

250 **Transcription of *PRX44* increases with ACC treatment driving ROS accumulation and ethylene-**
251 **induced root hair initiation**

252 The *ein3/eil1* transcription factor mutant has reduced root hair initiation and a reduction in PO1
253 signal in trichoblasts suggesting that there is transcriptional regulation of ROS producing enzymes that
254 drive root hair initiation. We examined a previously published microarray time course experiment in roots

255 treated with ACC (Harkey et al., 2018) to identify candidate transcriptional targets profiling the expression
256 pattern of transcripts encoding both ROS producing enzymes and proteins linked to trichoblast cell
257 specification. ROP2, ROPGEF3, ROPGEF4, GL2, RSL4 and RHD6, which are linked to root hair initiation
258 (Denninger et al., 2019), showed no transcriptional response to ACC treatment and primers that recognize
259 RSL1 and RSL2 are not present on the microarray and could not be examined in this dataset (Table S1).
260 A number of transcripts encoding class III PRXs changed in abundance in response to ACC, including the
261 transcript encoding *PRX44,* which increased by 3-fold. Class III peroxidases are specific to plants and exist
262 in large multigene families. They have been implicated in root hair tip growth, as null mutants have shorter
263 root hairs compared to wild type (Mangano et al., 2017). Recent work has shown that auxin induces
264 expression of genes encoding four class III peroxidases (PRX), which results in an increase in both root
265 hair length and ROS accumulation (Mangano et al., 2017), however, the role of ethylene signaling in
266 regulating class III PRX expression to modulate root hair initiation or elongation has not been reported.

267 We examined control and ACC-treated seedlings harboring the *PRX44* promoter driving GFP and
268 examined GFP expression via LSCM. Seedlings treated with ACC showed a statistically significant >2-fold
269 increase in GFP fluorescence, suggesting that the *PRX44* promoter is induced downstream of ethylene
270 signaling (Figure 6A-B). We also asked whether these peroxidases participate in ACC-regulated root hair
271 initiation. We examined root hair numbers via light microscopy in Col-0 and *prx44-2* seedlings treated with
272 and without ACC. There were significantly fewer root hairs in *prx44-2* controls compared to Col-0 controls
273 and the effect of ACC on root hair initiation was reduced in the *prx44-2* mutant, although there was still a
274 significant response to ACC (Figure 6C-D). The root hairs in the ACC-treated mutant were also significantly
275 shorter compared to Col-0, which is consistent with the phenotype that has been reported in response to
276 auxin treatment (Figure 6E) (Mangano et al., 2017). When PO1 accumulation patterns were examined via
277 LSCM, we observed no significant increase in PO1 accumulation in hair cells of *prx44-2* seedlings treated
278 with ACC (Figure 6F-G). We also examined *prx73-4*, since the transcripts encoding PRX73 has also been
279 reported to be induced with auxin treatment to drive root hair elongation (Mangano et al., 2017) and these
280 transcripts profound increases in response to ACC treatment (Table S1). The *prx73-4* mutant showed no
281 change in PO1 fluorescence in the presence or absence of ACC as compared to Col-0 (Figure S3) and
282 showed no changes in root hair initiation after ACC treatment. These combined data indicate that the class

283 III PRX44 is transcriptionally regulated by ethylene and contributes to ethylene induced ROS accumulation
284 and root hair initiation.

285 **DISCUSSION**

286 Ethylene is a key hormonal regulator of root hair initiation and elongation (Guzman and Ecker,
287 1990; Kieber et al., 1993). Although the proteins that drive ethylene signaling are well characterized, the
288 downstream proteins that control the root hair developmental processes have received less study. Reactive
289 oxygen species (ROS) are critical for both root hair initiation and elongation (Foreman et al., 2003;
290 Gayomba and Muday, 2020; Jones et al., 2007; Takeda et al., 2008). In root hairs, one source of ROS is
291 the NADPH oxidase (NOX)/respiratory burst oxidase homolog C (RBOHC) that is localized to root hairs to
292 facilitate cell wall loosening and subsequent tip focused Ca^{2+} accumulation leading to cell elongation
293 (Foreman et al., 2003). The plant hormone auxin also increases ROS accumulation to drive root hair
294 elongation (Mangano et al., 2017), so we asked if ROS is a signaling molecule in ethylene-induced root
295 hair development. In this study, we examined the effects of ethylene signaling on root hair initiation and
296 ROS accumulation to determine if increased ethylene drives root hair initiation through regulation of ROS
297 producing enzymes and subsequent ROS accumulation in trichoblasts from which root hairs form.

298 We asked whether ethylene signaling induced root hair initiation at the root tip by examining root
299 hair number of Col-0 grown in the presence of low concentration of ethylene gas (0.5 ppm) and the ethylene
300 precursor, ACC (1 μM), for 4 hours in both Col-0 and ethylene signaling mutant seedlings. There was an
301 increase in the number of trichoblasts that formed root hairs in ethylene and ACC treated seedlings
302 compared to untreated controls. This root hair induction was most pronounced in a region starting 500 μm
303 from the root tip and ending at 1000 μm, which we refer to as zone 2. Consistent with this effect occurring
304 through ACC conversion to ethylene, the ACC induction in root initiation is lost in ethylene insensitive
305 mutants *etr1-3* and *ein3eil1*, consistent with our prior reports (Harkey et al., 2018) that showed that ACC-
306 inhibited root elongation, gravitropism, and lateral root formation are lost in the ethylene insensitive *ein2-5*
307 and *etr1-3* mutants at this dose of ACC under our growth conditions (Harkey et al., 2018; Lewis et al., 2011;
308 Negi et al., 2010). These findings are also consistent with efficient conversion of ACC to ethylene and ACC
309 effects root hair initiation due to ethylene signaling responses. A recent report described the ectopic

310 formation of root hairs when seedlings were treated with 10ppm ethylene for 2 days (Qiu et al., 2021). We
311 do not see this response after our short 4-hour treatment with 20-fold less ethylene.

312 We asked whether ACC and ethylene treatment increased ROS levels in wild-type seedlings using
313 both genetic and chemical ROS probes. Using a ratiometric reporter of ROS-induced gene expression,
314 ZAT12p-ROS, we found that in ACC-treated roots, ROS dependent gene expression was increased in a
315 region spanning from 500-1000 µm from the root tip (zone 2) in ACC treated roots compared to untreated
316 controls. We also examined the effect of ethylene and ACC on hydrogen peroxide using a boronate based
317 hydrogen peroxide selective sensor, PO1. Both ethylene and ACC lead to elevated H_2O_2 accumulation in
318 the trichoblast cells in zone 2 after 4 hours of treatment, but PO1 signal was at constant low levels in
319 atrichoblast cells. Consistent with this increasing ROS driving root hair formation, there was a significant
320 increase in PO1 signal within 2 hours after ACC treatment, prior to the initiation of root hair bulges. These
321 data are consistent with ROS acting downstream of ethylene signaling in zone 2 of the root, and that these
322 signals occur prior to root hair initiation.

323 We next asked which components of the ethylene signaling pathway were required for ethylene-
324 induced ROS synthesis in trichoblasts of zone 2. ROS accumulation was monitored in two *etr1* mutants: a
325 constitutive ethylene signaling *etr1-7* allele and an ethylene insensitive *etr1-3*, as well as the TF null mutant
326 *ein3eil1.* Compared to Col-0, *etr1-7* exhibited an increase in ROS accumulation and root hair number in the
327 presence and absence of ACC treatment, while these responses were lost in the ACC-treated ethylene
328 insensitive *etr1-3* and *ein3eil1* mutants. These results are consistent with the ethylene receptor ETR1 and
329 the EIN3/EIL1 master transcriptional regulators being required for ethylene-induced ROS accumulation and
330 root hair initiation and with ACC acting through this canonical ethylene signaling pathway.

331 To determine if RBOH/NOXs were contributing to ethylene-induced ROS synthesis, we asked
332 whether the RBOHC enzyme was required to drive ROS accumulation and root hair initiation. Based on
333 previous work detailing the role of RBOHC in root hair initiation and growth (Foreman et al., 2003; Gayomba
334 and Muday, 2020), we asked whether this enzyme was contributing to ethylene-induced ROS accumulation
335 and subsequent root hair initiation and/or elongation. ACC treated *rhd2-6*, which is an *RBOHC* null mutant,
336 had reduced ROS accumulation in trichoblasts compared to Col-0 and ACC failed to increase the number

337 of initiated root hairs and to increase root hair elongation. The abundance of RBOHC transcripts showed
338 small changes in response to ACC treatment (Harkey et al., 2018), while there was more than a 2-fold
339 increase in RBOH activity in response to ACC treatment and there was a 3-fold reduction in activity in the
340 *rhd2-6* (*rbohc*) mutant. These data suggest that ethylene signaling induces superoxide production in roots
341 via increases in RBOHC enzyme activity to drive root hair initiation and elongation. However, since there is
342 still some ACC induction of root hair initiation in the *rhd2-6* mutant, these data suggest that initiation may
343 require additional proteins.

344 We examined previously published ACC and ethylene transcriptomic datasets to search for
345 transcripts encoding root hair specification proteins and ROS producing enzymes that are ethylene
346 regulated. Although ACC did not change abundance of transcripts encoding ROP2, ROPGEF3, ROPGEF4,
347 GL2, RHD6, or RSL4, we identified several transcripts encoding class III peroxidase enzymes that showed
348 substantial increase in response to ACC. *PRX44 and PRX73*, showed a significant increase in abundance
349 after 4 hours of ACC treatment. We examined a PRX44 promoter driven GFP fusion protein (*pPRX44*::GFP)
350 observing its expression in trichoblast cells in zone 2 and demonstrated that ACC treatment leads to
351 significant increases in fluorescence intensity compared to untreated controls and that this expression is
352 localized to root hair cells. ACC treatment of the null mutant *prx73-4* and *prx44-2* led to decreased ROS
353 accumulation in root hair forming trichoblasts in *prx44-2* and no effect in *prx73-4* as compared to Col-0. The
354 decreased PO1 signal in *prx44-2* was accompanied by significant reductions in the number of root hairs
355 formed in this same root region and the length of these root hairs. Together these experiments implicate
356 Class III peroxidase enzymes in ethylene-regulated root hair initiation.

357 These peroxidase enzymes have also been implicated in regulation of root hair elongation, as null
358 mutants treated with auxin have shorter root hairs and less ROS compared to wild type (Mangano et al.,
359 2017). A recent report demonstrated that PRX enzymes function to modify the localization of extension
360 proteins to control cell wall structure to allow increased elongation in response to auxin (Javier Martinez
361 Pacheco, 2021). Class III peroxidases are specific to plants and exist in large multigene families. Reverse
362 genetic studies have shown that they are involved in lignification, cell elongation, stress defense and seed
363 germination (Shigeto and Tsutsumi, 2016). At least 73 Arabidopsis genes encode class III peroxidases,

364 however, due to their redundancy and lack of information on their substrate specificity, their functions and
365 mechanisms of regulation are relatively unclear. They are secreted into the cell wall or surrounding medium
366 and are involved in a number of different reactions that involve both ROS consumption and production
367 (Liszkay et al., 2003; Passardi et al., 2005). However, previous work regarding peroxidase activity in root
368 hair elongation suggests that they act as ROS producers, as 3 PRXs have been reported to be involved in
369 increasing the ROS gradient required for root hair elongation (Mangano et al., 2017).

370 To summarize our findings on ethylene-dependent root hair initiation via increased ROS synthesis
371 and to tie these findings with other studies, we present a model in Figure 7. Low dose and short 4-hour
372 treatments with ACC led to efficient conversion of ACC to ethylene by roots to initiate an ethylene signaling
373 cascade. Ethylene acts through the ETR1 receptor and the canonical signaling pathway to increase the
374 activity of EIN3/EIL1 TFs. EIN3/EIL1 binds to the root hair specific TF RHD6 to induce RSL4 expression
375 and root hair elongation (Feng et al., 2017). Root hair growth is controlled by several proteins that eventually
376 activate the RHD6 TF. Downstream of RHD6, the RSL4 TF is activated and it defines final root hair length
377 based on its level of expression (Datta et al., 2015; Mangano et al., 2017). Previous work has shown that
378 EIN3 physically interacts with RHD6 to form a transcriptional complex that coactivate RSL4 to promote root
379 hair elongation (Feng et al., 2017), and that EIN3 and RSL4 both act to downregulate GL2 expression to
380 drive ectopic root hair formation with long term treatments with high levels of ethylene (Qiu et al., 2021).
381 However, in our microarray dataset (Harkey et al., 2018), *RSL4* transcript abundance only showed slight
382 changes in response to ACC treatment (Table S1). It has also been shown that auxin treatment results in
383 increased RSL4 transcript abundance, which binds to the promoters of RBOH and four class III peroxidase
384 (*PRX*) genes, including *PRX44*, to drive ROS synthesis in root hair cells. RSL4 activation via auxin induces
385 class III peroxidase and *RBOH* expression, which leads to ROS accumulation required to drive root hair
386 elongation (Mangano et al., 2017). We find that ACC treatment increases activity of RBOHC enzymes
387 leading to increased ROS and root hair elongation, without changing the abundance of *RBOHC* transcripts.
388 Additionally, ACC treatment leads to the transcriptional regulation of class III peroxidases (Harkey et al.,
389 2018), resulting in ROS production and root hair initiation. Further investigation regarding the mechanisms
390 of ethylene-regulated ROS synthesis is required. For example, one important question to be answered is
391 how ethylene signaling regulates RBOH activity. This could occur through a number of different

392 mechanisms, such as calcium binding or phosphorylation, which are known to regulate RBOH enzymes
393 (Postiglione and Muday, 2020). It is also unknown as to whether ethylene regulates class III peroxidase
394 expression via EIN3 or an alternate transcriptional mechanism, or if ethylene also regulates class III
395 peroxidase enzyme activity.

396

397 **MATERIALS AND METHODS**

398 **Growth conditions and root hair quantification**

399 All Arabidopsis mutants were in the Col-0 background. The *etr1-7*, *etr1-3* (AT1G66340), *ein3-1*
400 (AT3G20770) *eil1-1* (AT2G27050) double and *rhd2-6* (AT5G51060) mutants have all been described
401 previously (Binder et al., 2007; Gayomba and Muday, 2020; Harkey et al., 2018; Hua and Meyerowitz,
402 1998). The ZAT12p-ROS construct was generously provided by Won-Gyu Choi (Lim et al., 2019). *prx44-2*
403 (AT4G06010) and *prx73-4* (AT5G67400) were obtained from the Arabidopsis SALK center
404 (SALK_057222C and SALK_020724, respectively), the mutations were verified by PCR, and homozygous
405 lines were isolated. The transcriptional reporter *pPRX44*::GFP transgenic line was described previously
406 (Marzol, 2021). Seeds were sterilized in 70% ethanol for approximately 5 minutes and grown on 100 x 15
407 mm Petri dishes containing 25 mL media. Seedlings were grown on 1x MS supplemented with 1% sucrose,
408 vitamins (1 µg/ml thiamine, 0.5 µg/ml pyridoxine and 0.5 µg/ml nicotinic acid), 0.05% MES (w/v) and 0.8%
409 (w/v) agar. Media pH was 5.5. Micropore tape was used to seal the top of the Petri dish and plated seeds
410 were stratified at 4◦ C in darkness for 2 days. Plants were grown under 24h light from T5 fluorescent lights
411 at 120-150 µmol photons m^{-2} s^{-1}.

412 **Quantification of root hair number and root hair length**

413 Seedlings were grown for 5 days on control media and then transferred to media containing 1 µM
414 ACC and grown for 4 hours or other indicated times. To examine root hairs, 5-day old seedlings were
415 imaged using bright-field on an Axio Zoom V16 stereomicroscope. Extended depth of focus was used to
416 combine z-stack images. Root hairs that were at stage +1 or +2 (or later stages) as defined by (Denninger
417 et al., 2019) were quantified using Fiji/ImageJ software in three zones (0-500 µm, 500-1000 µm, 1000-1500
418 µm) starting from the root tip.

419 We also determined root hair length in the presence and absence of ACC treatment in Col-0 ad
420 mutants. All root hairs in zone 2 that had begun to elongate (were at stages above +2) were measured
421 using Fiji/ImageJ software. The length of each root in microns was determined. To obtain the histogram of
422 distribution, the roots were separated into bins of different lengths, and the % of root hairs in each length
423 bin was determined by dividing by the total number of root hairs in Zone 2 in that root.

424 **Confocal imaging of dyes and reporters of ROS levels**

425 H_2O_2 was visualized with Peroxy-Orange 1 (PO1). PO1 was dissolved in DMSO to make a 500 µM
426 stock and was further diluted in H_2O to make a 50 µM working solution. Seedlings were incubated in PO1
427 for 15 minutes in the dark and were then rinsed with H_2O and mounted in H_2O for imaging. Control, ACC-
428 treated and ethylene-treated seedlings were imaged on a Zeiss 880 laser scanning confocal microscope
429 using a 10x objective. PO1 was excited with a 488 nm laser at 0.25% power and emission was collected
430 between 544-695 nm. Images were analyzed using Fiji/ImageJ software. Plot profiles were taken across
431 the epidermal cell files of maximum intensity projections using a 20-pixel line and values were averaged
432 within each cell file.

433 5-day old seedlings harboring the ZAT12p-ROS construct were mounted in H_2O and excited with
434 488 and 561 nm lasers at 6% and 1.2% laser power, respectively. GFP emission was collected at 521 nm
435 and mCherry emission was collected at 593 nm. Fiji/ImageJ software was used to generate two single
436 channel images to form individual GFP and mCherry channels. Plot profiles were taken using a 250-pixel
437 wide line to measure fluorescence of the entire root. Measurements were taken starting at 200 µm back
438 from the root tip and ending at 1500 µm. Ratios were generated by dividing the GFP channel by mCherry
439 using the Image Calculator tool (Process/Image Calculator).

440 **PI staining and *proPRX44*::GFP imaging**

441 Cell walls were stained with 0.5 µg/mL propidium iodide (PI) dissolved in H_2O. 5 day old seedlings
442 treated with and without ACC were incubated in PI for 4 minutes before imaging. Fluorescence was
443 visualized using a 561 nm laser at 0.15% and emission spectra set to 561-695 nm. These settings were
444 used for all images. Optical slices of the top section of the root to show epidermal cells and maximum
445 intensity projections of z-stack images are shown in Figure S1. Fiji software was used to measure cell
446 length of 3 epidermal cells per root using optical slices of the top section of the root. Cells were chosen at
447 the bottom of zone 2 (cell 1, in the middle (cell 2), and at the top (cell 3). 4 cells of each of the 3 cell types
448 were averaged and are shown in FS1. 6-8 roots of both control and ACC treated seedlings. Transgenic
449 seeds harboring *pPRX44*::GFP were obtained from the lab of Dr. Jose Estevez, 5-day old seedlings were

450 mounted in H_2O and excited with a 488 nm laser at 5% and emission was collected between 490-606 nm.
451 Seedlings were then stained with PI.

452 **DNA extraction and PCR for mutant genotype analysis**

453 T-DNA insertion lines were grown for approximately 2 weeks on media described above, then
454 transferred to soil and grown under 24h light at 50-80 µmol photons m^{-2} s^{-1}. Leaves were harvested from 6
455 week old plants and stored in eppendorf tubes at -20° C prior to DNA extraction. Frozen leaves were ground
456 in DNA extraction buffer (100 mM Tris-HCl pH 8.0, 10 mM Na2EDTA, 100 mM $LiCl_2$, 1% (w/v) SDS).
457 Samples were then washed once with isopropanol and three times with 80% (v/v) ethanol. Finally, DNA
458 pellets were dried, resuspended in sterile H_2O and stored at -20° C. Each PCR reaction contained 1X GoTaq
459 Polymerase, 1 µM of each primer, 1 uL of DNA and 5 µL H_2O. To confirm that mutants were homozygous
460 for the desired T-DNA insertion, one reaction was performed with primers (left primer and right primer)
461 flanking the left and right sides of in-tact genes while one reaction was performed with the right primer and
462 LBb1.3, which is a primer specific for the left border of the T-DNA insertion. PCR products were run on 0.8
463 % (w/v) agarose gels containing 0.002% SERVA DNA stain G.

464 **NADPH oxidase/RBOH enzyme assays**

465 Protein extract was isolated from seedlings grown on a nylon filter as described previously (Harkey
466 et al., 2018). After 2 days of stratification and 7 days of growth under conditions described above, the nylon
467 was transferred to growth medium with and without 1 µM ACC for 4 hours. Roots were then cut from
468 seedlings and flash frozen in liquid nitrogen. Frozen samples were ground in liquid nitrogen using a mortar
469 and pestle. RBOH extraction buffer (50 mM Tris-HCl pH 7.5, 0.1 mM EDTA, 0.1% (v/v) Triton X-100, 1 mM
470 $MgCl_2$, 10% (v/v) glycerol) was then added to a plant material/buffer ratio of 1:3 (w/v). Samples were
471 centrifuged and supernatant was collected and desalted and concentrated using the Amicon Ultra-0.5
472 Centrifugal Filter devices. RBOH reaction mixture (50 mM Tris-HCl pH 7.5, 1 mM $CaCl_2$, 0.1 mM nitroblue
473 tetrazolium (NBT), 0.1 mM NADPH) was then mixed with protein extract at a 1:1 ratio. The reduction of
474 NBT to monoformazan was monitored spectrophotometrically at 530 nm. Monoformazan concentrations
475 were calculated using a 12.8 $mM^{-1}cm^{-1}$ extinction coefficient. This assay was adapted in sweet peppers and
476 has previously been described (Chu-Puga et al., 2019).

ACKNOWLEDGMENTS

We would like to thank Dr. Brad Binder (University of Tennessee) and all Muday lab members for their editorial input, and Dr. Glen Marrs and Dr. Heather Brown-Harding (Wake Forest University) for their help with microscopy.

COMPETING INTERESTS

The authors have no competing interests.

FUNDING

This project was supported by the National Science Foundation (MCB-1716279 to GKM) and a USDA Predoctoral Fellowship (NIFA 2021-67034-35113 to REM). Dr. Jose Estevez and Dr. Eliana Marzol are investigators of the National Research Council (CONICET) from Argentina supported by grants from ANPCyT (PICT2019-0015 to J.M.E. and PICT2018-0577 to E.M.) and ANID – Programa Iniciativa Científica Milenio ICN17_022 and Fondo Nacional de Desarrollo Científico y Tecnológico [1200010] to J.M.E.

DATA AVAILABILITY

All data in this manuscript are included in the text or in the supplementary file.

491 **REFERENCES**

492 Alonso, J.M., Hirayama, T., Roman, G., Nourizadeh, S., Ecker, J.R., 1999. EIN2, a bifunctional transducer of
493 ethylene and stress responses in Arabidopsis. Science 284, 2148-2152.
494 Berger, F., Haseloff, J., Schiefelbein, J., Dolan, L., 1998. Positional information in root epidermis is defined
495 during embryogenesis and acts in domains with strict boundaries. Curr Biol 8, 421-430.
496 Bienert, G.P., Moller, A.L.B., Kristiansen, K.A., Schulz, A., Moller, I.M., Schjoerring, J.K., Jahn, T.P., 2007.
497 Specific aquaporins facilitate the diffusion of hydrogen peroxide across membranes. J Biol Chem 282,
498 1183-1192.
499 Binder, B.M., 2020. Ethylene signaling in plants. J Biol Chem 295, 7710-7725.
500 Binder, B.M., Walker, J.M., Gagne, J.M., Emborg, T.J., Hemmann, G., Bleecker, A.B., Vierstra, R.D., 2007.
501 The Arabidopsis EIN3 binding F-box proteins EBF1 and EBF2 have distinct but overlapping roles in
502 ethylene signaling. Plant Cell 19, 509-523.
503 Bleecker, A.B., 1999. Ethylene perception and signaling: an evolutionary perspective. Trends Plant Sci 4,
504 269-274.
505 Bruex, A., Kainkaryam, R.M., Wieckowski, Y., Kang, Y.H., Bernhardt, C., Xia, Y., Zheng, X.H., Wang, J.Y., Lee,
506 M.M., Benfey, P., Woolf, P.J., Schiefelbein, J., 2012. A Gene Regulatory Network for Root Epidermis
507 Cell Differentiation in Arabidopsis. Plos Genet 8.
508 Carroll, A.D., Moyen, C., Van Kesteren, P., Tooke, F., Battey, N.H., Brownlee, C., 1998. Ca2+, annexins, and
509 GTP modulate exocytosis from maize root cap protoplasts. Plant Cell 10, 1267-1276.
510 Chao, Q.M., Rothenberg, M., Solano, R., Roman, G., Terzaghi, W., Ecker, J.R., 1997. Activation of the
511 ethylene gas response pathway in Arabidopsis by the nuclear protein ETHYLENE-INSENSITIVE3 and
512 related proteins. Cell 89, 1133-1144.
513 Chapman, J.M., Muhlemann, J.K., Gayornba, S.R., Muday, G.K., 2019. RBOH-Dependent ROS Synthesis and
514 ROS Scavenging by Plant Specialized Metabolites To Modulate Plant Development and Stress
515 Responses. Chem Res Toxicol 32, 370-396.
516 Chu-Puga, A., Gonzalez-Gordo, S., Rodriguez-Ruiz, M., Palma, J.M., Corpas, F.J., 2019. NADPH Oxidase
517 (Rboh) Activity is Up Regulated during Sweet Pepper (Capsicum annuum L.) Fruit Ripening.
518 Antioxidants-Basel 8.
519 Datta, S., Prescott, H., Dolan, L., 2015. Intensity of a pulse of RSL4 transcription factor synthesis
520 determines Arabidopsis root hair cell size. Nat Plants 1.
521 De Baets, S., Denbigh, T.D.G., Smyth, K.M., Eldridge, B.M., Weldon, L., Higgins, B., Matyjaszkiewicz, A.,
522 Meersmans, J., Larson, E.R., Chenchiah, I.V., Liverpool, T.B., Quine, T.A., Grierson, C.S., 2020. Micro-
523 scale interactions between Arabidopsis root hairs and soil particles influence soil erosion. Commun
524 Biol 3.
525 Denninger, P., Reichelt, A., Schmidt, V.A.F., Mehlhorn, D.G., Asseck, L.Y., Stanley, C.E., Keinath, N.F., Evers,
526 J.F., Grefen, C., Grossmann, G., 2019. Distinct RopGEFs Successively Drive Polarization and Outgrowth
527 of Root Hairs. Curr Biol 29, 1854-+.
528 Di Cristina, M., Sessa, G., Dolan, L., Linstead, P., Baima, S., Ruberti, I., Morelli, G., 1996. The Arabidopsis
529 Athb-10 (GLABRA2) is an HD-Zip protein required for regulation of root hair development. Plant J 10,
530 393-402.
531 Dickinson, B.C., Huynh, C., Chang, C.J., 2010. A Palette of Fluorescent Probes with Varying Emission Colors
532 for Imaging Hydrogen Peroxide Signaling in Living Cells. J Am Chem Soc 132, 5906-5915.
533 Dolan, L., Duckett, C.M., Grierson, C., Linstead, P., Schneider, K., Lawson, E., Dean, C., Poethig, S., Roberts,
534 K., 1994. Clonal Relationships and Cell Patterning in the Root Epidermis of Arabidopsis. Development
535 120, 2465-2474.
536 Feng, Y., Xu, P., Li, B.S., Li, P.P., Wen, X., An, F.Y., Gong, Y., Xin, Y., Zhu, Z.Q., Wang, Y.C., Guo, H.W., 2017.
537 Ethylene promotes root hair growth through coordinated EIN3/EIL1 and RHD6/RSL1 activity in
538 Arabidopsis. P Natl Acad Sci USA 114, 13834-13839.

539 Foreman, J., Demidchik, V., Bothwell, J.H.F., Mylona, P., Miedema, H., Torres, M.A., Linstead, P., Costa, S.,
540 Brownlee, C., Jones, J.D.G., Davies, J.M., Dolan, L., 2003. Reactive oxygen species produced by NADPH
541 oxidase regulate plant cell growth. Nature 422, 442-446.
542 Galway, M.E., Masucci, J.D., Lloyd, A.M., Walbot, V., Davis, R.W., Schiefelbein, J.W., 1994. The Ttg Gene Is
543 Required to Specify Epidermal-Cell Fate and Cell Patterning in the Arabidopsis Root. Dev Biol 166, 740-
544 754.
545 Gayomba, S.R., Muday, G.K., 2020. Flavonols regulate root hair development by modulating accumulation
546 of reactive oxygen species in the root epidermis. Development 147.
547 Grebe, M., 2012. The patterning of epidermal hairs in Arabidopsis - updated. Curr Opin Plant Biol 15, 31-
548 37.
549 Guzman, P., Ecker, J.R., 1990. Exploiting the Triple Response of Arabidopsis to Identify Ethylene-Related
550 Mutants. Plant Cell 2, 513-523.
551 Harkey, A.F., Watkins, J.M., Olex, A.L., DiNapoli, K.T., Lewis, D.R., Fetrow, J.S., Binder, B.M., Muday, G.K.,
552 2018. Identification of Transcriptional and Receptor Networks That Control Root Responses to
553 Ethylene. Plant Physiol 176, 2095-2118.
554 Harkey, A.F., Yoon, G.M., Seo, D.H., DeLong, A., Muday, G.K., 2019. Light Modulates Ethylene Synthesis,
555 Signaling, and Downstream Transcriptional Networks to Control Plant Development. Front Plant Sci 10.
556 Hua, J., Meyerowitz, E.M., 1998. Ethylene responses are negatively regulated by a receptor gene family in
557 Arabidopsis thaliana. Cell 94, 261-271.
558 Javier Martinez Pacheco, P.R., Luciana Kasulin, Corina M. Fusari, Lucas Servi, Lucía Ferrero, Victoria
559 Berdion Gabarain, Juan Manuel Peralta, Cecilia Borassi, Eliana Marzol, Diana Rosa Rodríguez-Garcia,
560 Yossmayer del Carmen Rondón Guerrero, Mariana Carignani Sardoy, Javier Botto, Claudio Meneses,
561 Federico Ariel, Ezequiel Petrillo, Christophe Dunand, José M. Estevez, 2021. Apoplastic class III
562 peroxidases PRX62 and PRX69 regulate ROS-homeostasis and cell wall associated extensins linked to
563 root hair growth at low-temperature in Arabidopsis thaliana. Nature Communications in press.
564 Jones, M.A., Raymond, M.J., Yang, Z.B., Smirnoff, N., 2007. NADPH oxidase-dependent reactive oxygen
565 species formation required for root hair growth depends on ROP GTPase. J Exp Bot 58, 1261-1270.
566 Ju, C.L., Yoon, G.M., Shemansky, J.M., Lin, D.Y., Ying, Z.I., Chang, J.H., Garrett, W.M., Kessenbrock, M.,
567 Groth, G., Tucker, M.L., Cooper, B., Kieber, J.J., Chang, C., 2012. CTR1 phosphorylates the central
568 regulator EIN2 to control ethylene hormone signaling from the ER membrane to the nucleus in
569 Arabidopsis. P Natl Acad Sci USA 109, 19486-19491.
570 Kieber, J.J., Rothenberg, M., Roman, G., Feldmann, K.A., Ecker, J.R., 1993. Ctr1, a Negative Regulator of
571 the Ethylene Response Pathway in Arabidopsis, Encodes a Member of the Raf Family of Protein-
572 Kinases. Cell 72, 427-441.
573 Kobayashi, M., Ohura, I., Kawakita, K., Yokota, N., Fujiwara, M., Shimamoto, K., Doke, N., Yoshioka, H.,
574 2007. Calcium-dependent protein kinases regulate the production of reactive oxygen species by potato
575 NADPH oxidase. Plant Cell 19, 1065-1080.
576 Kwak, J.M., Mori, I.C., Pei, Z.M., Leonhardt, N., Torres, M.A., Dangl, J.L., Bloom, R.E., Bodde, S., Jones,
577 J.D.G., Schroeder, J.I., 2003. NADPH oxidase AtrbohD and AtrbohF genes function in ROS-dependent
578 ABA signaling in Arabidopsis. Embo J 22, 2623-2633.
579 Leavitt, R., 1904. Trichomes of the root of vascular cryptograms and angiosperms. Proceedings of the
580 Boston Society of Natural History 31, 273-313.
581 Lee, M.M., Schiefelbein, J., 1999. WEREWOLF, a MYB-related protein in arabidopsis, is a position-
582 dependent regulator of epidermal cell patterning. Cell 99, 473-483.
583 Lewis, D.R., Negi, S., Sukumar, P., Muday, G.K., 2011. Ethylene inhibits lateral root development, increases
584 IAA transport and expression of PIN3 and PIN7 auxin efflux carriers. Development 138, 3485-3495.

585 Lim, S.D., Kim, S.H., Gilroy, S., Cushman, J.C., Choi, W.G., 2019. Quantitative ROS bioreporters: A robust
586 toolkit for studying biological roles of ROS in response to abiotic and biotic stresses. Physiol Plantarum
587 165, 356-368.
588 Liszkay, A., Kenk, B., Schopfer, P., 2003. Evidence for the involvement of cell wall peroxidase in the
589 generation of hydroxyl radicals mediating extension growth. Planta 217, 658-667.
590 Mangano, S., Denita-Juarez, S.P., Choi, H.S., Marzol, E., Hwang, Y., Ranocha, P., Velasquez, S.M., Borassi,
591 C., Barberini, M.L., Aptekmann, A.A., Muschietti, J.P., Nadra, A.D., Dunand, C., Cho, H.T., Estevez, J.M.,
592 2017. Molecular link between auxin and ROS-mediated polar growth. P Natl Acad Sci USA 114, 5289-
593 5294.
594 Marzol, E., Borassi, C., Ranocha, P., Aptekman, A.A., Bringas, M., Pennington, J., Paez-Valencia, J., Pacheco,
595 J.M., Garcia, D.R.R., Guerrero, Y.D.C, Carignani, M., Mangano, S., Fleming, M., Mishler-Elmore, J.W.,
596 Blanco-Herrera, F., Bedinger, P., Dunand, C., Capece, L., Nadra, A.D., Held, M., Otegu, M., Estevez, J.M,
597 2021. Class III peroxidases PRX01, PRX44, and PRX73 potentially target extensins during root hair
598 growth in Arabidopsis thaliana.
599 Masucci, J.D., Schiefelbein, J.W., 1994. The Rhd6 Mutation of Arabidopsis-Thaliana Alters Root-Hair
600 Initiation through an Auxin-Associated and Ethylene-Associated Process. Plant Physiol 106, 1335-1346.
601 Masucci, J.D., Schiefelbein, J.W., 1996. Hormones act downstream of TTG and GL2 to promote root hair
602 outgrowth during epidermis development in the Arabidopsis root. Plant Cell 8, 1505-1517.
603 Mittler, R., Vanderauwera, S., Suzuki, N., Miller, G., Tognetti, V.B., Vandepoele, K., Gollery, M., Shulaev,
604 V., Van Breusegem, F., 2011. ROS signaling: the new wave? Trends Plant Sci 16, 300-309.
605 Molendijk, A.J., Bischoff, F., Rajendrakumar, C.S.V., Friml, J., Braun, M., Gilroy, S., Palme, K., 2001.
606 Arabidopsis thaliana Rop GTPases are localized to tips of root hairs and control polar growth. Embo J
607 20, 2779-2788.
608 Negi, S., Sukumar, P., Liu, X., Cohen, J.D., Muday, G.K., 2010. Genetic dissection of the role of ethylene in
609 regulating auxin-dependent lateral and adventitious root formation in tomato. Plant J 61, 3-15.
610 Passardi, F., Cosio, C., Penel, C., Dunand, C., 2005. Peroxidases have more functions than a Swiss army
611 knife. Plant Cell Rep 24, 255-265.
612 Pemberton, L.M.S., Tsai, S.L., Lovell, P.H., Harris, P.J., 2001. Epidermal patterning in seedling roots of
613 eudicotyledons. Ann Bot-London 87, 649-654.
614 Poole, L.B., Schoneich, C., 2015. Introduction: What we do and do not know regarding redox processes of
615 thiols in signaling pathways. Free Radical Bio Med 80, 145-147.
616 Postiglione, A.E., Muday, G.K., 2020. The Role of ROS Homeostasis in ABA-Induced Guard Cell Signaling.
617 Front Plant Sci 11.
618 Qiu, Y., Tao, R., Feng, Y., Xiao, Z., Zhang, D., Peng, Y., Wen, X., Wang, Y., Guo, H., 2021. EIN3 and RSL4
619 interfere with an MYB-bHLH-WD40 complex to mediate ethylene-induced ectopic root hair formation
620 in Arabidopsis. Proc Natl Acad Sci U S A 118.
621 Rerie, W.G., Feldmann, K.A., Marks, M.D., 1994. The Glabra2 Gene Encodes a Homeo Domain Protein
622 Required for Normal Trichome Development in Arabidopsis. Gene Dev 8, 1388-1399.
623 Salazar-Henao, J.E., Velez-Bermudez, I.C., Schmidt, W., 2016. The regulation and plasticity of root hair
624 patterning and morphogenesis. Development 143, 1848-1858.
625 Schiefelbein, J., Huang, L., Zheng, X.H., 2014. Regulation of epidermal cell fate in Arabidopsis roots: the
626 importance of multiple feedback loops. Front Plant Sci 5.
627 Schiefelbein, J.W., Somerville, C., 1990. Genetic-Control of Root Hair Development in Arabidopsis-
628 Thaliana. Plant Cell 2, 235-243.
629 Shibata, M., Sugimoto, K., 2019. A gene regulatory network for root hair development. J Plant Res 132,
630 301-309.
631 Shigeto, J., Tsutsumi, Y., 2016. Diverse functions and reactions of class III peroxidases. New Phytol 209,
632 1395-1402.

633 Solano, R., Stepanova, A., Chao, Q.M., Ecker, J.R., 1998. Nuclear events in ethylene signaling: a
634 transcriptional cascade mediated by ETHYLENE-INSENSITIVE3 and ETHYLENE-RESPONSE-FACTOR1.
635 Gene Dev 12, 3703-3714.
636 Suzuki, N., Miller, G., Morales, J., Shulaev, V., Torres, M.A., Mittler, R., 2011. Respiratory burst oxidases:
637 the engines of ROS signaling. Curr Opin Plant Biol 14, 691-699.
638 Takeda, S., Gapper, C., Kaya, H., Bell, E., Kuchitsu, K., Dolan, L., 2008. Local positive feedback regulation
639 determines cell shape in root hair cells. Science 319, 1241-1244.
640 Tanimoto, M., Roberts, K., Dolan, L., 1995. Ethylene is a positive regulator of root hair development in
641 Arabidopsis thaliana. Plant J 8, 943-948.
642 Wen, X., Zhang, C.L., Ji, Y.S., Zhao, Q., He, W.R., An, F.Y., Jiang, L.W., Guo, H.W., 2012. Activation of
643 ethylene signaling is mediated by nuclear translocation of the cleaved EIN2 carboxyl terminus. Cell Res
644 22, 1613-1616.

645

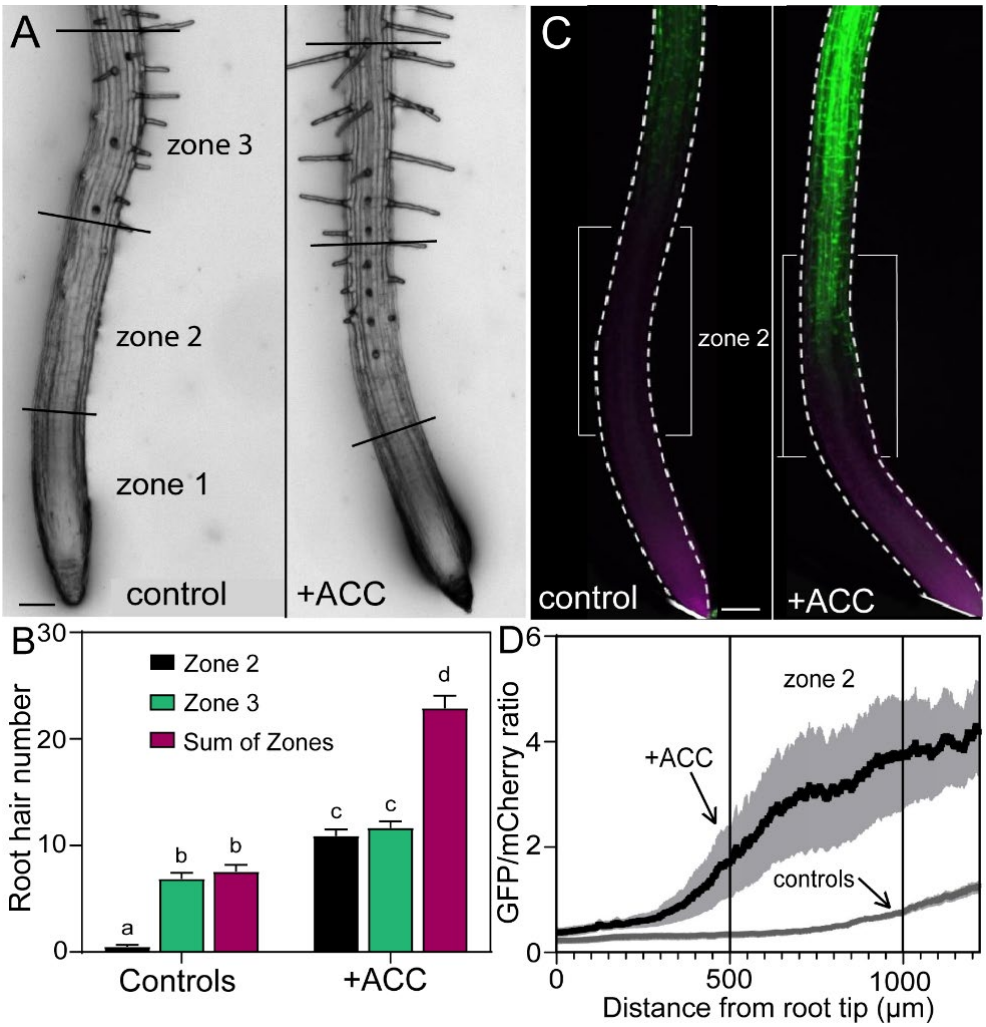

Figure 1. ACC treatment induced root hair number and ROS dependent gene expression along the root after 4 hours (A) Representative images of root tips in Col-0 treated with and without ACC for 4 hours. Zones 1, 2, and 3 represent 500 µm root sections. Scale bar for all images are 100 µm. (B) Root hair quantification of untreated and 4h ACC treated seedlings. No root hairs formed in zone 1. Data are means ± SEM of total RH in zone 2, zone 3, and all zones from 3 experiments (n=18-24 seedlings per experiment). Columns with different letters indicate statistically significant differences determined by two-way ANOVA followed by Tukey's multiple comparisons test. (C) Representative images of root tips of Col-0 containing the ZAT12p-ROS reporter treated with or without ACC for 4 hours with GFP signal in green and mCherry signal in magenta. White brackets indicate zone 2 of the root. (D) Quantification of the ratio of GFP/mCherry fluorescence intensity using a line profile along the roots of an average of 6-12 seedlings of 3 independent experiments of untreated or ACC treated seedlings. Data are means ± SEM.

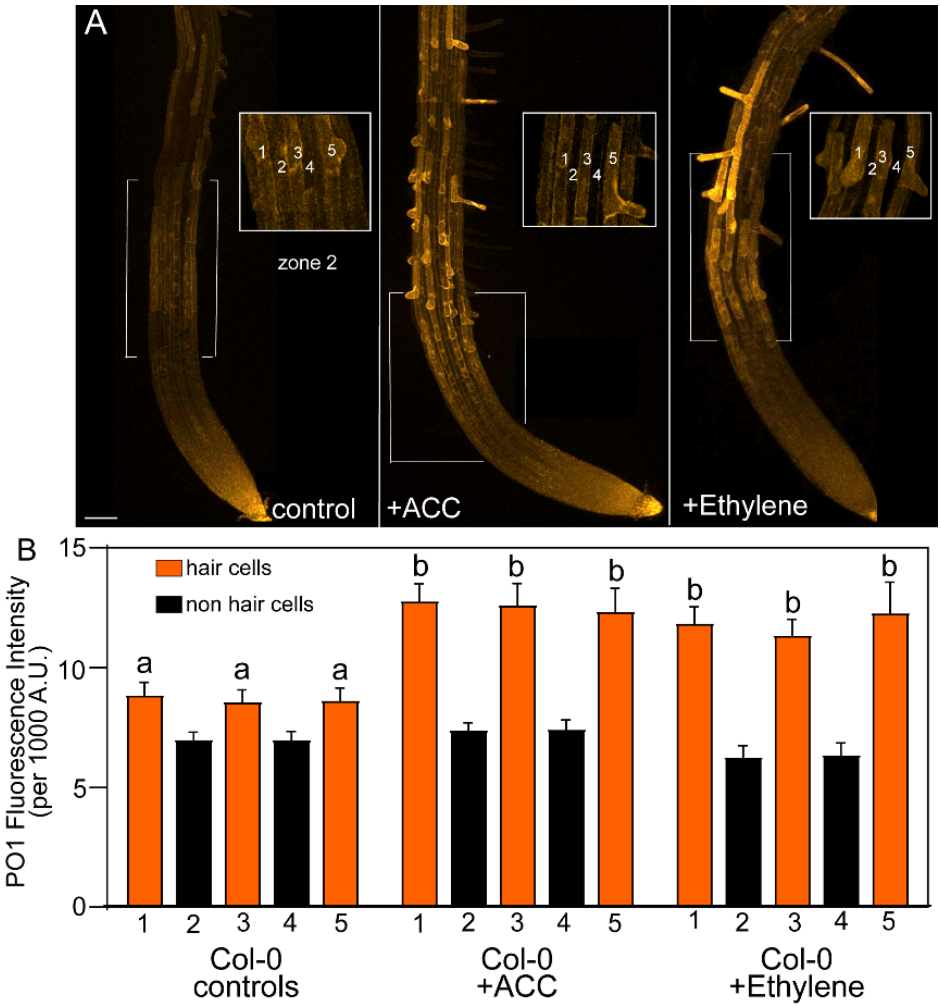

Figure 2. ACC and ethylene gas increase H_2O_2 accumulation in trichoblasts after 4 hours. (A) Representative roots illustrating the alternating PO1 fluorescence between trichoblast and atrichoblast epidermal cell files of cells in Col-0 roots with and without ACC and ethylene gas treatment for 4 hours. White brackets indicate zone 2 of the root. Inset indicates hair cells (1, 3, 5) vs. non hair cells (2, 4). (B) Quantification of PO1 fluorescence intensity in trichoblasts (orange bars: 1, 3 and 5) and atrichoblasts (black bars: 2, 4). Data are means ± SEM of 3 independent experiments (n=18-24 seedlings/experiment). Columns with different letters indicate statistical significance compared to Col-0 untreated cells as determined by two-way ANOVA followed by Tukey's multiple comparisons test.

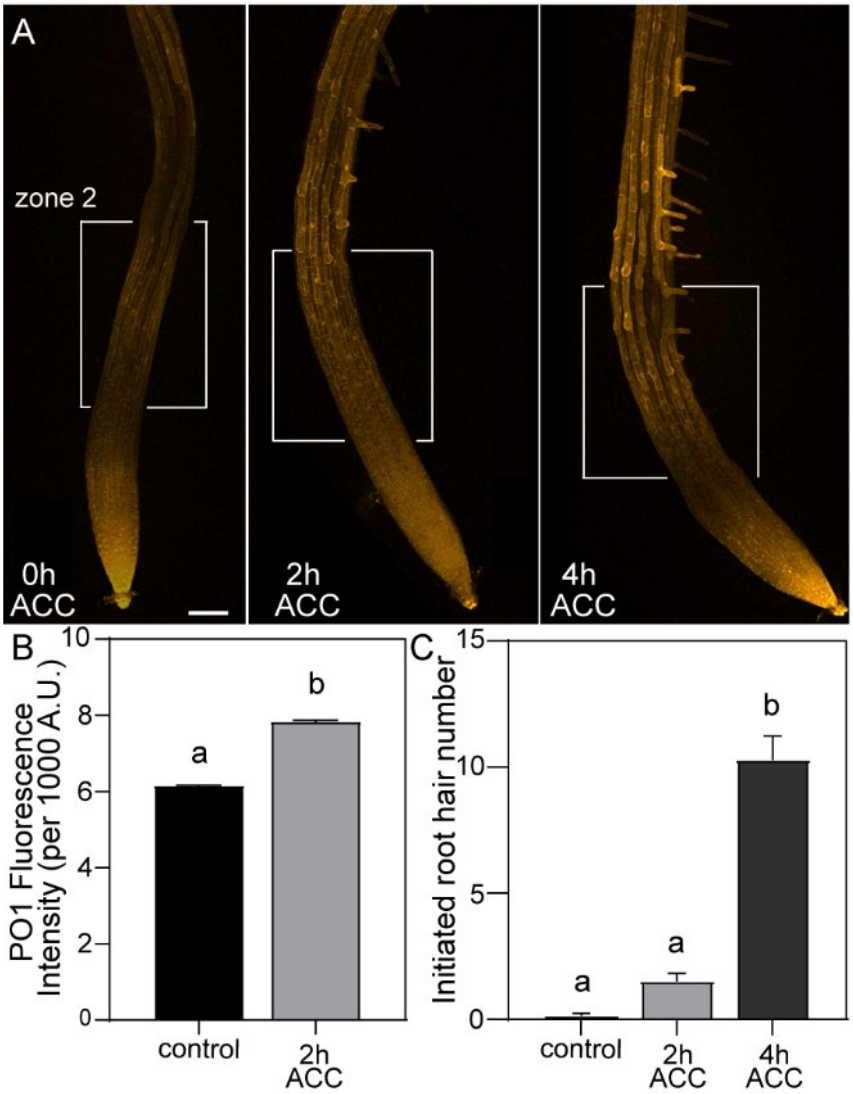

Figure 3. Ethylene-induced ROS accumulation preceded root hair initiation. (A) Representative images of epidermal PO1 fluorescence in untreated Col-0 and Col-0 treated with ACC for 2 or 4h. Scale bar is 100 µm. White brackets indicate zone 2 of the root. (B) Quantification of trichoblasts that had not yet formed root hair bulges of control and 2h ACC treated seedlings. (C) Quantification of number of initiated root hairs in zone 2 of the root (500 µm-1000 µm from root tip) in untreated and 2 and 4h ACC-treated seedlings. Data are mean ± SEM of individual cells from 3 independent experiments (n= 12-18 seedlings/experiment). Columns with different letters indicate statistical significance compared to untreated hair cells as determined by Student's t-test ($p < 0.0001$) in B. Columns with different letters indicate statistically significant differences determined by one-way ANOVA followed by Tukey's multiple comparisons test in C.

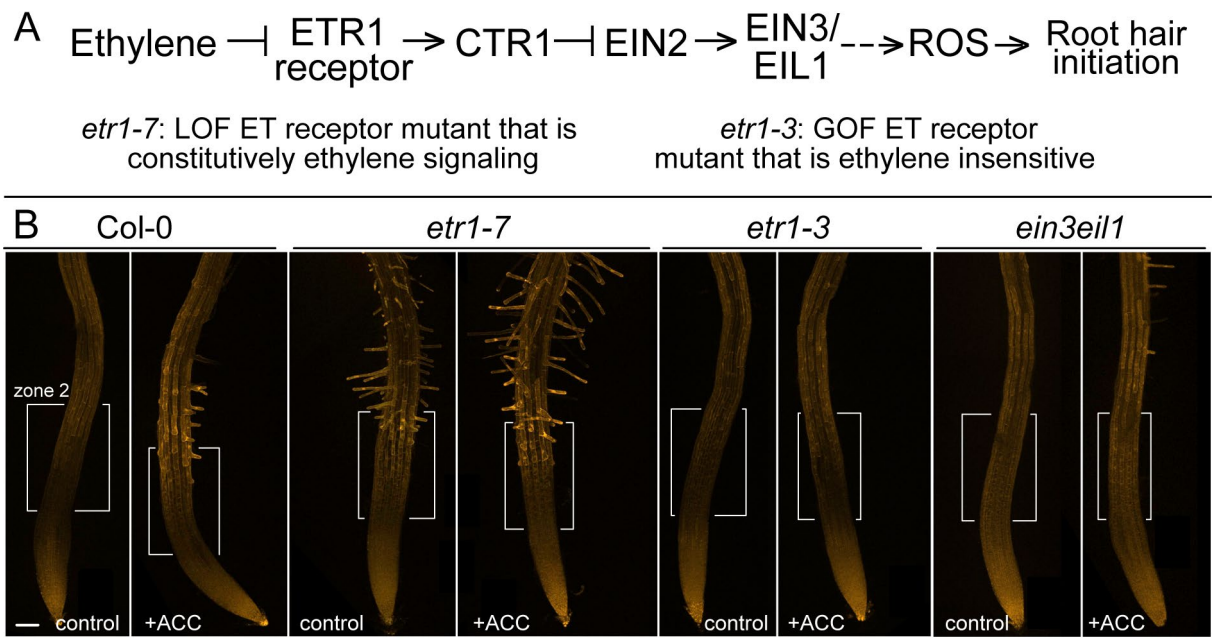

Figure 4. The ETR1 receptor and EIN3/EIL1 transcription factors are required for ethylene-induced ROS accumulation and root hair proliferation. (A) A schematic diagram of the ethylene signaling pathway and explanation of the character of the *etr* mutants. ETR1 (ethylene resistant 1) is the ethylene receptor controlling root hair formation, CTR1 (constitutive triple response 1 is a kinase, EIN2 (ethylene insensitive 2) is a signaling protein, EIN3 and EIL1 (EIN3-like 1) are transcription factors. (B) Representative images of PO1 epidermal fluorescence in Col-0, *etr1-7*, *etr1-3*, and *ein3-1eil1-1* treated with and without ACC for 4 hours. 18-20 seedlings from each genotype and treatment were imaged. Scale bar is 100 µm.

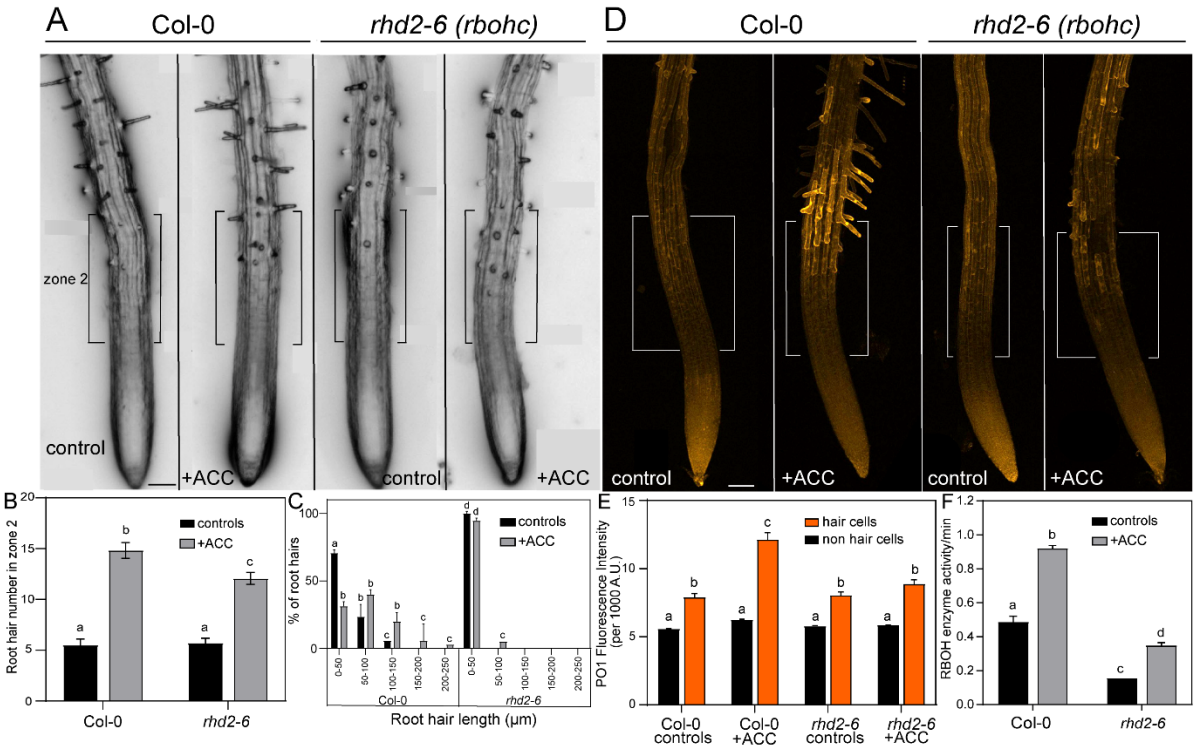

Figure 5. RBOHC activity contributes to ethylene-induced ROS accumulation. (A) Representative images of root hairs of Col-0 and *rhd2-6* treated with and without ACC for 4 hours. Black brackets indicate zone 2 of the root. (B) Root hair quantification of untreated and 4h ACC treated seedlings. Data are means ± SEM of total RH in zone 2 from 3 experiments (n=18-24 seedlings per experiment). Columns with different letters indicate statistically significant differences determined by two-way ANOVA followed by Tukey's multiple comparisons test. (C) Quantification of percent of root hairs within a certain micron length of Col-0 and *rhd2-6* treated with and without ACC. Columns with different letters indicate statistically significant differences determined by two-way ANOVA followed by Tukey's multiple comparisons test. (D) Representative images of PO1 epidermal fluorescence in Col-0 and *rhd2-6* treated with and without ACC for 4 hours. White brackets indicate zone 2 of the root. (E) Quantification of PO1 fluorescence intensity in hair cells and non-hair cells. For each root PO1 fluorescence was quantified in two hair cells (cells 1 and 5 from Figure 2) and two nonhair cells (cells 2 and 4 from Figure 2) and the values pooled to obtain this average. Data are means ± SEM of 3 experiments (n=18-24 seedlings/experiment). Columns with different letters indicate statistical significance in PO1 signal compared to other hair cells as determined by two-way ANOVA followed by Tukey's multiple comparisons test. (F) Quantification of formazan concentration per

700 minute in roots of Col-0 and *rhd2-6* treated with and without ACC for 4 hours. Data are means ± SEM of 3
701 experiments. Columns with different letters indicate statistical significance as determined by two-way
702 ANOVA followed by Tukey's multiple comparisons test. Scale bars for all images are 100 μm.

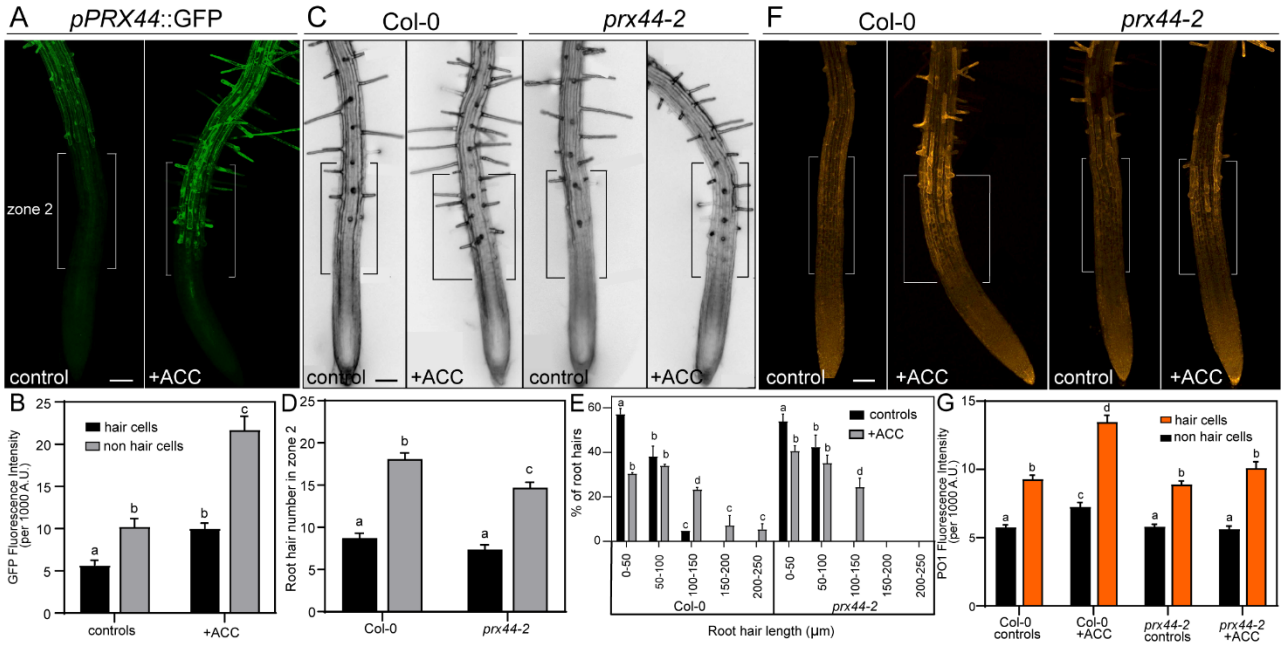

Figure 6. *pPRX44*::GFP expression increases in roots treated with ACC and PRX44 contributes to ethylene-induced root hair formation and H_2O_2 accumulation in root hair cells (A) Representative images of *pPRX44*::GFP treated with and without ACC for 4 hours. White brackets indicate zone 2 of the root. (B) Quantification of GFP signal in hair and non-hair cells of *pPRX44*::GFP treated with and without ACC. Data are means ± SEM (C) Representative images of RH number in Col-0 and *prx44-2* treated with and without ACC for 4 hours. Black brackets indicate zone 2 of the root. (D) Root hair quantification of untreated and 4h ACC treated seedlings. Data are means ± SEM. of 3 independent experiments (n=18-24 seedlings per experiment). Columns with different letters indicated statistically significant differences determined by two-way ANOVA followed by Tukey's multiple comparison test. (E) Quantification of percent of root hairs within a certain micron length of Col-0 and *prx44-2* treated with and without ACC. Columns with different letters indicate statistically significant differences determined by two-way ANOVA followed by Tukey's multiple comparisons test. (F) Representative images of Col-0 and *prx44-2* treated with and without ACC for 4 hours and stained with PO1. White brackets indicate zone 2 of the root. (G) Quantification of PO1 accumulation in hair and non-hair cells of Col-0 and *prx44-2* treated with and without ACC for 4 hours (n=12-18 seedlings per experiment). For each root PO1 fluorescence was quantified in two hair cells (cells 1 and 5 from Figure 2) and two nonhair cells (cells 2 and 4 from Figure 2) and the values pooled to obtain this average.Data are means ± SEM of 3 experiments. Columns with different letters indicate

720 statistical significance compared to all other hair cells as determined by two-way ANOVA followed by
721 Tukey's multiple comparisons test. Scale bars for all images are 100 μm.

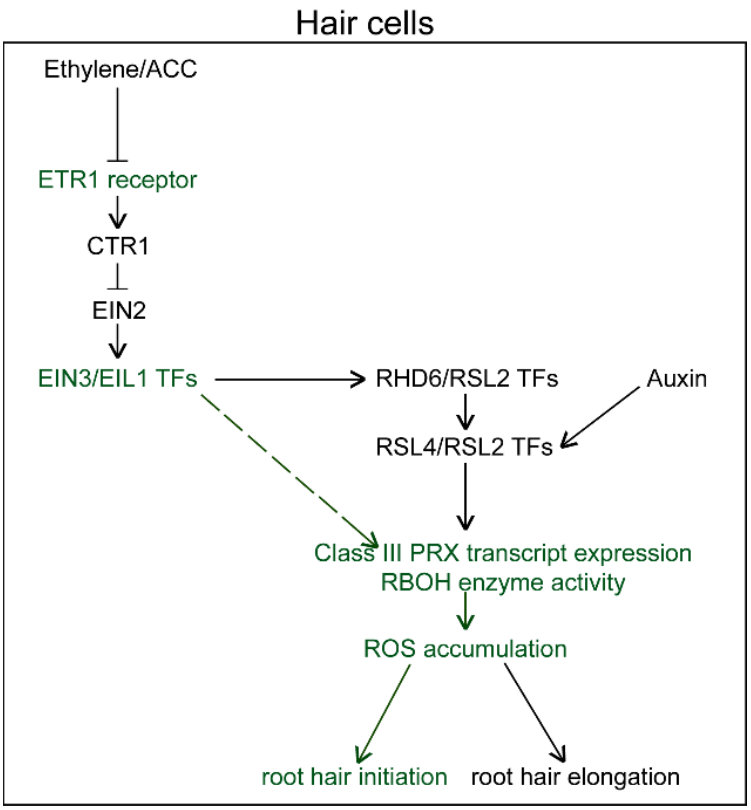

723 **Figure 7. Summary of mechanisms by which ethylene and auxin modulate ROS and root hair**
724 **formation**. In hair cells, ethylene, acting through the ETR1 receptor and the canonical ethylene signaling
725 pathway induces accumulation of EIN3/EIL1 TF proteins. Previous work has shown that EIN3/EIL1
726 physically interacts with RHD6/RSL2 TFs to induce expression of RSL4/RSL2 transcripts leading to root
727 hair elongation (Feng et al., 2017). It has also been shown that RSL4/RSL2 is induced by auxin signaling
728 and that RSL4/RSL2 binds to the promoters of RBOH and class III PRX genes to induce transcript
729 expression and root hair elongation (Mangano et al., 2017). Here, highlighted in green, we have shown that
730 ethylene signaling through ETR1 and EIN3/EIL1 induces ROS accumulation through RBOHC enzyme
731 activity and PRX44 transcript expression to drive root hair initiation.